Thermodynamic spin magnetization of strongly correlated two-dimensional electrons in a silicon inversion layer

O. Prus,[1] Y. Yaish,[1] M. Reznikov,[1] U. Sivan,[1] and V. Pudalov[2]
[1]*Department of Physics and Solid State Institute, Technion-IIT, Haifa 32000, Israel*
[2]*P. N. Lebedev Physics Institute, 119991 Moscow, Russia*
(Received 18 November 2002; published 9 May 2003)

A method invented to measure the minute thermodynamic magnetization of dilute two-dimensional fermions is applied to electrons in a silicon inversion layer. The interplay between the ferromagnetic interaction and disorder enhances the low temperature susceptibility up to 7.5 folds compared with the Pauli susceptibility of noninteracting electrons. The magnetization peaks in the vicinity of the density, where transition to strong localization takes place. At the same density, the susceptibility approaches the free spins value (Curie susceptibility), indicating an almost perfect compensation of the kinetic energy toll associated with spin polarization by the energy gained from the Coulomb correlation. Yet, the balance favors a paramagnetic phase over spontaneous magnetization in the whole density range.

DOI: 10.1103/PhysRevB.67.205407 PACS number(s): 71.30.+h, 73.20.Fz, 73.40.Qv

I. INTRODUCTION

The nature of the ground state of degenerate two-dimensional (2D) fermions at zero magnetic field is an outstanding open problem, which has not been deciphered despite decades of research. In the absence of disorder the ground state is believed to be determined by an interplay between the kinetic energy E_F and the interparticle interaction energy $E_c = e^2/\kappa a$, where $a = (\pi n)^{-1/2}$ is the inter particle distance, n is the areal particle density, and κ is the host dielectric constant. The relative importance of the two energy scales is characterized by $r_s = a/a_0$, with a_0 being the Bohr radius. For electrons in a single band $r_s = E_c/E_F$, while for the (100) surface of silicon $r_s = E_c/2E_F$ due to the twofold valley degeneracy. At very high densities ($r_s \ll 1$) a 2D system approaches the noninteracting degenerate gas paramagnetic limit, characterized by the Pauli susceptibility χ_0. As the density is reduced, the growing ferromagnetic correlations lead to substantial enhancement of the spin susceptibility χ. The system is predicted to remain paramagnetic up to $r_s \approx 20-25$, where numerical calculations[1,2] find a quantum phase transition to a ferromagnetic liquid phase.[3] At lower density $r_s \approx 37$,[4] the Coulomb correlations are predicted to lead via another phase transition to a quantum Wigner crystal with frustrated antiferromagnetic spin arrangement[5] followed by transition to a ferromagnetic arrangement at an even lower density.[6] The energy balance between the ferromagnetic and paramagnetic states is very subtle and the density window where ferromagnetism may take place is small.[1,2] Such a ferromagnetic phase has never been observed experimentally. The situation is fundamentally complicated by the unavoidable disorder present in any realistic system. In the absence of Coulomb interactions all wave functions of a 2D system are believed to be exponentially localized.[7] Localization modifies the Coulomb interaction dramatically in the low density limit. The interplay between kinetic energy, interaction, and disorder was worked out theoretically for the case of relatively weak disorder.[8–10] It was found that the interaction suppresses the localizing effect of disorder, especially in the presence of valley degeneracy.[11] Yet, at low enough densities disorder prevails and localization always commences.

Notwithstanding the substantial research done thus far, there is presently no agreed picture of the phase diagram corresponding to a realistic 2D fermion system. It is clear that the spin degree of freedom plays a crucial role in the low density regime $n \leqslant 2 \times 10^{11}$ cm^{-2} but the minute total magnetic moment pertaining to such a small number of spins has hindered, thus far, any direct measurement of the thermodynamic spin magnetization. Present estimates of the 2DEG magnetization in silicon rely on susceptibility data obtained from transport measurements, either Shubnikov–de Haas (Sh-dH) oscillations in a tilted magnetic field[12–15] or saturation of the magnetoresistance in an in-plane field.[16,17] The two approaches led to contradicting conclusions. While the magnetoresistance data were interpreted as indicating the long awaited Bloch-Stoner[3] instability at the critical density for the metal-insulator transition, analysis of Sh-dH oscillations points against such instability.[18]

At the heart of the present manuscript is a method used to measure the thermodynamic magnetization directly. We apply the method to a high mobility 2D electron layer in silicon. In particular, we find that, as the density is reduced, the weak field spin susceptibility is progressively enhanced up to 7.5 χ_0, but the ferromagnetic instability is never realized. The system turns insulating before it polarizes and electron localization then leads to a reduction in the Coulomb interaction. The localization transition is thus characterized by a sharp cusp in magnetization. Interestingly, we find indications for localized magnetic moments in coexistence with the itinerant electrons, even at high carrier densities.

II. METHOD, SAMPLES, AND EXPERIMENTAL SETUP

The experimental setup is presented in Fig. 1. An external bias V_G sets a constant electrochemical potential difference between the gate and the 2D channel equal to the sum of the

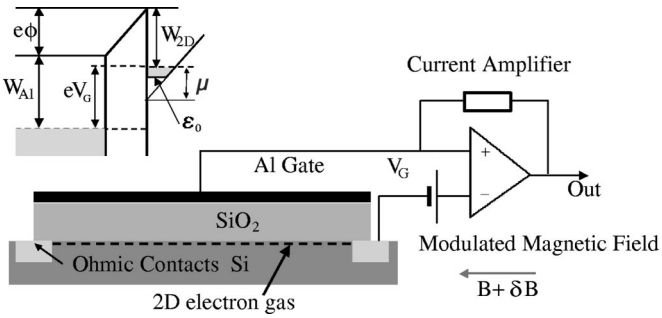

FIG. 1. Magnetization measurement setup and band diagram of the 2D confining potential.

electrostatic potential difference, ϕ, and the difference between the aluminum gate and the 2DEG work functions, W_{Al} and $W_{2\mathrm{D}}$, respectively,

$$eV_G = e\phi(n) + W_{\mathrm{Al}} - W_{2\mathrm{D}}(n,B). \tag{1}$$

Modulation of the in-plane magnetic field by an auxiliary coil at a frequency ω modulates the chemical potential of the 2DEG and, hence, $W_{2\mathrm{D}}$ (W_{Al} modulation is negligible). Since V_G is kept constant, the differential of Eq. (1) vanishes. The 2DEG chemical potential μ equals the Si-SiO_2 band discontinuity minus $W_{2\mathrm{D}}$ (Fig. 1). Consequently, one obtains

$$e\frac{\partial\phi}{\partial n}dn + \frac{\partial\mu}{\partial n}dn + \frac{\partial\mu}{\partial B}dB = 0 \tag{2}$$

or

$$\frac{\partial\mu}{\partial B} = -\left(e\frac{\partial\phi}{\partial n} + \frac{\partial\mu}{\partial n}\right)\frac{dn}{dB}, \tag{3}$$

where $(e\partial\phi/\partial n + \partial\mu/\partial n)/e^2 = C^{-1}$ is the independently measured inverse capacitance per unit area, comprising the geometrical and chemical potential contributions. The latter contribution includes well width and interaction effects.

In terms of the induced current δI and the magnetic field modulation δB one obtains

$$\frac{\partial\mu}{\partial B} = -\frac{ie\,\delta I}{C\omega\,\delta B}. \tag{4}$$

Since the 2D layer thickness and the screening length are minuscule compared with the oxide thickness, the capacitance is close to the geometrical one, and hence, constant to within 1% in the whole density range. Using one of Maxwell's relations $\partial M/\partial n = -\partial\mu/\partial B$, we obtain $\partial M/\partial n$ and integrate it numerically with respect to n to derive the magnetization $M(B,n)$. The magnetic susceptibility χ is calculated from the slope of $M(B,n)$ versus B at small fields. An additional constant field, induced by the main coil, facilitates magnetization measurements at finite magnetic field.

While the method is conceptually straightforward, its realization is demanding since the current induced by the field modulation is typically on the order of 10^{-15} A, while the spurious current induced in all wire loops by the ac magnetic field, and even more so by mechanical vibrations of the sample in the dc magnetic field, are potentially larger by several orders of magnitude. The induced currents were minimized in the experiment by careful compensation of all loops. Mechanical vibrations were minimized by rebuilding the relevant parts of the refrigerator to achieve high enough mechanical rigidity. After building several prototypes we were able to drive all mechanical resonances to frequencies considerably higher than the field modulation frequency and, hence, eliminate the mechanical vibrations at the measurement frequency.

The same setup can be used to measure the much larger orbital magnetization in a perpendicular magnetic field. The method's sensitivity scales with sample's area and magnetic field modulation amplitude. For the 4 mm^2 sample and 0.03 T rms field modulation used here, it was about 10^{-14} J/T, comparable to the best sensitivity achieved with SQUID-based magnetometers[19] [a review of the current state of the art in magnetization measurements can be found in Ref. 20]. The advantage of our (and Ref. 19) method is in its applicability to arbitrary magnetic fields and temperatures, as well as to a wide range of conductivities. The extraction of the magnetization from Sh-dH oscillations, on the other hand, requires perpendicular magnetic fields, low temperatures and high enough mobilities. The most interesting regime, the transition to strong localization is, hence, at the limit of its reach.

The samples used in the experiment were similar to those used in Refs. 21,22. They consisted of 5 mm long 0.8 mm wide Hall bars with 2.5 mm separation between the potential probes. The oxide was 200 nm thick, leading to $C = 678$ pF device capacitance. We applied -15 V bias to the substrate in order to minimize the contacts resistance.[23] The maximal mobility under this bias reached 17,000 $\mathrm{cm}^2/\mathrm{V\,s}$. An alternating magnetic field of typically 100–300 Gs (rms) and $f = \omega/2\pi = 5$–20 Hz was applied parallel to the layer along with a desired constant field. A preamplifier with $\sim 2\,fA/\sqrt{Hz}$ current noise was used to measure the current and bias the gate (Fig. 1).

Unlike Sh-dH based measurements, our method is sensitive to the total thermodynamic magnetization comprising the spin part as well as the diamagnetic orbital contribution due to the finite (~ 50 Å) thickness of the 2D layer (Fig. 1). Localized states also contribute to the measured magnetization, as long as they exchange particles with the 2DEG at a rate faster than ω.

III. EXPERIMENTAL RESULTS AND DISCUSSION

The measured $\partial M/\partial n$ at 9 T magnetic field and $T = 100$ mK is depicted by dots in Fig. 2(a). The smooth solid line depicts the same quantity as extracted from Sh-dH data.[15] The difference between the two curves is attributed to the diamagnetic shift due to the sub-band energy level (ε_0 in Fig. 1) dependence upon the magnetic field and to the presence of localized spins. Both effects do not appear in Sh-dH oscillations. While the localized spins are certainly relevant

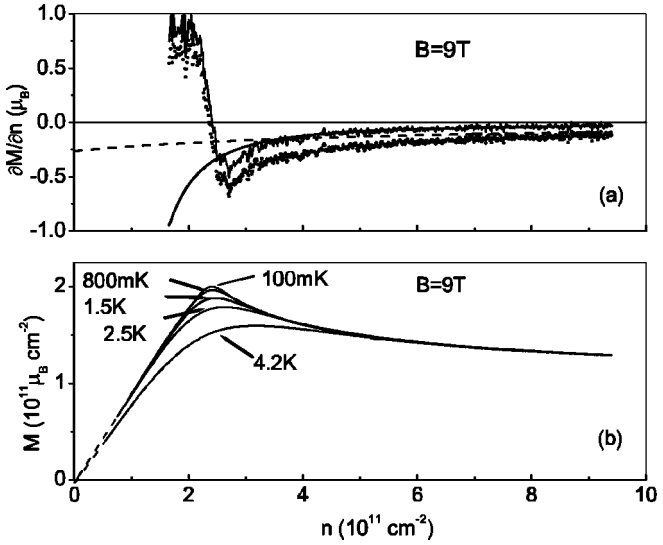

FIG. 2. (a) Total and spin $\partial M/\partial n$. Dots: measured total $\partial M/\partial n$, dashed line: diamagnetic contribution, thick smooth line: spin $\partial M/\partial n$ extracted from Sh-dH data (Ref. 15) thin solid line: spin $\partial M/\partial n$ extracted by subtraction of the diamagnetic contribution from the total $\partial M/\partial n$. (b) Spin magnetization obtained by integration of $\partial M/\partial n$ data. The dashed line demonstrates that the curves extrapolate to zero M at vanishing density, as they should.

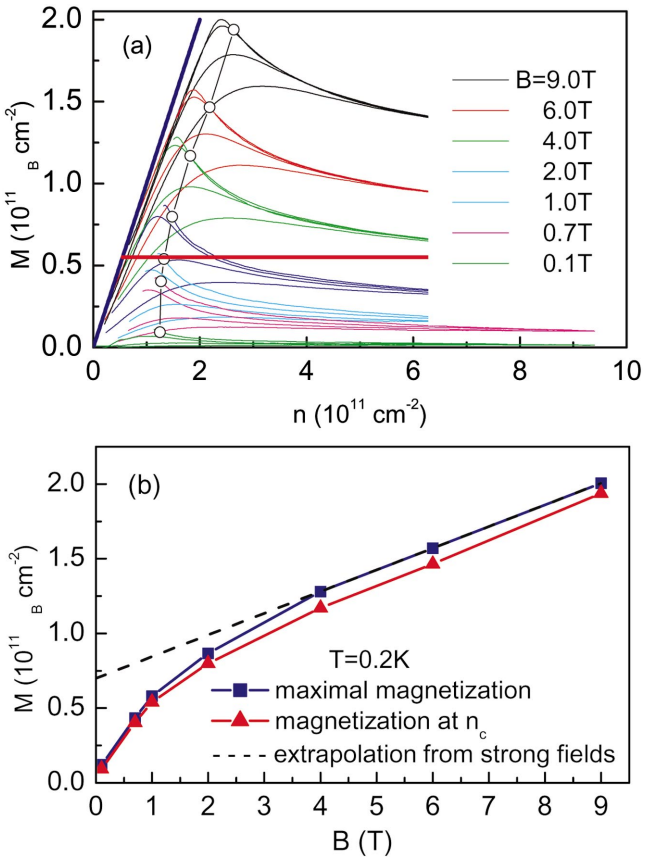

FIG. 3. (Color) (a) Spin magnetization as a function of density at different magnetic fields and temperatures 0.2, 0.8, 2.5, and 4.2 K; higher magnetization corresponds to lower temperature. Critical densities n_c are marked by circles. Thick blue line: full magnetization, thick red line: magnetization of a degenerate ideal electron gas at $B=6$ T. (b) Maximal spin magnetization and spin magnetization at the critical densities plotted against magnetic field. Dashed line: extrapolation from high magnetic fields.

to the study of spin magnetization in real samples, the diamagnetic part reflects an orbital effect, which is outside the scope of our interest. To estimate the latter contribution we assume that the Sh-dH measurements at high densities (say $n \geqslant 5\times10^{11}$ cm^{-2}), where the number of localized spins is small, give the spin magnetization correctly. The diamagnetic contribution is then given by the difference between our measured thermodynamic magnetization and the one extracted from the Sh-dH data. At zero density, on the other hand, one can calculate the diamagnetic shift in a single-particle picture. To complete the estimate at intermediate densities we interpolate between the two limits to obtain the dashed line in Fig. 2(a). The spin magnetization in the whole density range is obtained by subtraction of the diamagnetic contribution (dashed line) from the measured data (dots). The effect of the magnetic field, even at 9 T, on the subband energy ε_0 is much smaller than the intersubband spacing. Therefore, the diamagnetic contribution to the magnetization should depend linearly upon magnetic field, in accordance with our high density data. The overall diamagnetic contribution in the low-density range is small compared with the spin contribution. Moreover, it varies slowly with density. The extracted spin magnetization is therefore only slightly affected by the details of the interpolation procedure. Yet, for $n \leqslant 2\times10^{11}$ cm^{-2} we find that the saturation value of the extracted spin magnetization $\partial M/\partial n$ [solid line in Fig. 2(a)] is lower by $\approx 10\%$ than the one Bohr magneton per electron, expected for full polarization. Since all spins are likely to be polarized at low density and 9 T, we attribute the discrepancy to an underestimate of the diamagnetic contribution at low densities. The error in our measured data is much smaller than 10%. The magnetization values presented below may, hence, underestimate the actual magnetization at low densities by up to $2\times10^{9}\mu_B$ cm^{-2} per T. This uncertainty is immaterial for our conclusions. The rest of the paper focuses on the spin contribution obtained by the above procedure.

The spin magnetization [Fig. 2(b)] at a given field is obtained by numerical integration of the extracted $\partial M/\partial n$ values with respect to n. Since the magnetization can be measured only above a certain density, for which the sample resistance is lower than $\simeq 1$ MΩ, the integration cannot start from zero density, where $M=0$. Consequently, our integration yields the magnetization up to a constant, which is chosen so that the magnetization at high densities equals the values extracted from the Sh-dH oscillations. We neglect the small number of localized spins, which are present even at high densities. The fact that the resulting curves at all temperatures extrapolate to practically zero magnetization at $n=0$ [dashed lines in Fig. 2(b)] confirms that the integration constants are chosen properly.

The spin magnetization at various magnetic fields and four temperatures is depicted in Fig. 3(a). For each magnetic field the curves with higher magnetization values correspond to lower temperatures. The thick blue line corresponds to full

polarization of all carriers at a given density and the thick red line to the zero temperature magnetization of a noninteracting degenerate electron gas at $B=6$ T. The empty circles denote for each magnetic field the critical density $n_c(B)$, which separates the metallic regime from the insulating one.[24] At higher densities the resistance decreases as the temperature is reduced (metallic behavior) while at lower densities it increases (insulator). Whether the metallic behavior indicates a true 2D metal or merely finite temperature transport through localized states with long enough localization length is presently an open question. It is clear, though, that the insulating regime corresponds to localized states (either in the sense of percolation or in the sense of exponentially decaying wave functions) with progressively smaller localization lengths at lower densities. At high magnetic fields, full spin alignment persists up to densities considerably higher than those predicted for noninteracting electrons (compare the noninteracting and the experimental curves for $B=6$ T). Curiously, for all magnetic fields the magnetization reaches its maximal value at densities only slightly lower than the critical density n_c. As more carriers are added to the layer, the total magnetization is monotonically reduced. The large negative slope of the curves in the vicinity of n_c indicates that the added delocalized electrons prefer to occupy the upper spin subband. At still higher densities the magnetization is further reduced towards the respective noninteracting values.

Figure 3(b) depicts the maximal magnetization as well as the magnetization at the critical densities versus magnetic field. The data set an upper limit on the zero field polarization at the critical density $n_c \approx 1.25\times10^{11}$ cm^{-2}, to less than 2×10^{10} μ_B cm^{-2}. Our data, hence, point against Stoner instability in our samples.

Within effective medium theory the inverse susceptibility per particle assumes Curie-Weiss form $\chi=\mu_B^2/k_B(T-T_c)$. The value of T_c in this approximation provides an intuitive measure for the combined effects of the kinetic energy and interaction. In particular, a ferromagnetic instability requires positive T_c. The paramagnetic nature of the 2D layer should, hence, be reflected in the temperature dependence of the susceptibility χ. The inverse susceptibility, determined from $B=0.7$ T spin magnetization, normalized by the electron density and expressed in K is depicted as a function of temperature in Fig. 4. For all densities the inverse susceptibility per spin is larger (negative T_c) than the Curie value $\chi^{-1}=k_BT/\mu_B^2$, indicating that in the balance between the Coulomb energy gain and the kinetic energy toll associated with spin polarization in the system, the latter wins. Yet, at the lowest densities the victory is marginal, $T_c\cong0.2$ K. To appreciate the almost perfect balancing of the kinetic energy by the interaction, we compare the data for $n=8\times10^{10}$ cm^{-2} (thick line connecting the data points in Fig. 4) to the theoretical inverse susceptibility of a noninteracting 2D Fermi gas of the same density. The difference between the two curves reflects the effects of the ferromagnetic interaction and disorder, which are absent in an ideal noninteracting gas. Remarkably, the susceptibility measured at densities just below n_c, approaches the free spin one (Curie law) very closely, implying that the kinetic energy is almost perfectly

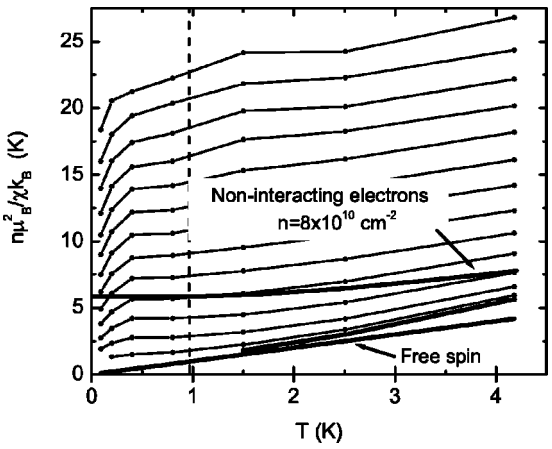

FIG. 4. Inverse susceptibility as determined from $M(B)$ at $B=0.7$ T. Experimental points from bottom to top correspond to densities 0.8–6×10^{11} cm^{-2} in 4×10^{10} cm^{-2} steps. The thick straight line depicts Curie law and the dashed line marks $T=(g\mu_B/k_B)\times0.7$ T. The experimental points at $n=8\times10^{10}$ are connected by a thick line for comparison with the expectation for noninteracting electrons of the same density.

compensated by the interaction. Yet, the former wins and paramagnetism prevails. Since we believe that the free spin-like susceptibility near the critical density is generic, rather than fortuitous, we propose that the localization transition is driven, in addition to disorder, by the strong exchange interaction, which promotes localization through the Pauli principle. Localization, in turn, reduces the overlap between the electron wave functions and, hence, the exchange interaction (a strongly localized system is believed to have a nearest neighbor antiferromagnetic order[25]). This scenario also explains the large positive magnetoresistance observed in the vicinity of the n_c.[26,27] Magnetic field aligns the spins, and again by the Pauli principle, drives the system towards the insulating phase. The localization transition at higher fields is, hence, shifted to higher densities. The proposed scenario also highlights the similarity between the localization transition in high mobility 2DEG and the Mott transition.[28]

Note, that in contrast to all expectations, χ in the metallic phase depends on temperature down to 0.1 K. This dependence indicates the existence of a relevant energy scale considerably smaller than the Zeeman one (dashed vertical line in Fig. 4). Such an energy scale may originate from localized spins which interact very weakly with each other. Quantification of the number of localized spins and their contribution to M (Ref. 29) requires further study.

Figure 5 depicts the magnetization vs magnetic field for various densities. The magnetization at densities close to n_c increases strongly with decreasing temperature. The magnetization is nonlinear, implying that sufficiently low magnetic fields are required (less than 0.7 T in our case) to determine the ''zero'' field susceptibility. At $T=100$ mK and $n=1.25\times10^{11}$ cm^{-2} the strong Coulomb interaction is manifested in a 7.5 folds enhancement of the susceptibility compared with noninteracting electrons. This susceptibility is twice as large as the value extracted from the Sh-dH data[15] for the same density. We attribute the difference to the localized states

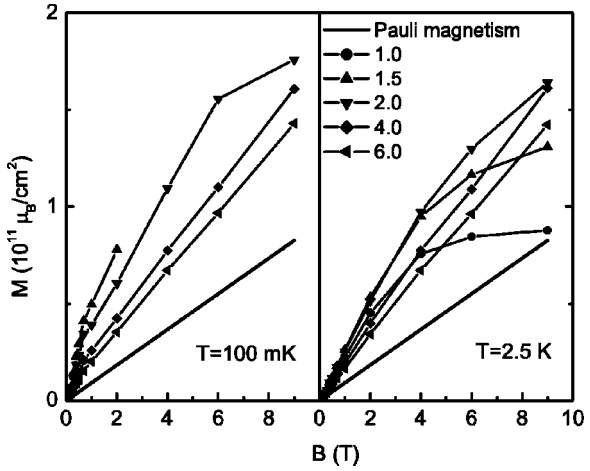

FIG. 5. Magnetization as a function of magnetic field at $T=100$ mK and $T=2.5$ K. Densities are given in 10^{11} cm^{-2} units. Bold line: Pauli magnetization for noninteracting degenerate fermions. As the temperature and magnetic field are reduced, the magnetization becomes increasingly nonlinear.

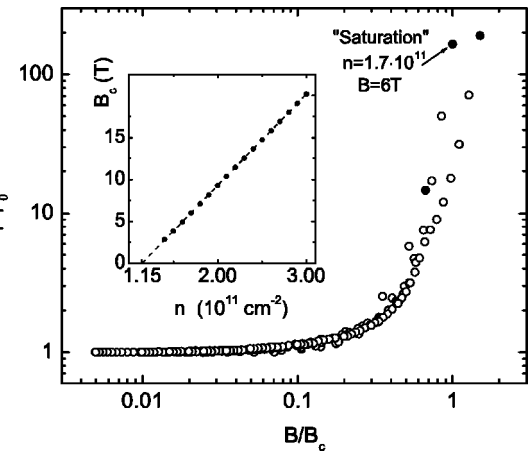

FIG. 6. Normalized magnetoresistance at different densities plotted versus scaled magnetic field $B/B_c(n)$. The field $B_c(n)$, used to scale the data, is shown by dots in the inset. The extrapolation of the scaling field to zero at a finite density, n_0, was used in Ref. 16 to claim a ferromagnetic instability at $n=n_0$.

which persist into the metallic phase $n>n_c$ and are not sensed by the Sh-dH analysis. The weak interaction between such spins should result in a very large susceptibility at low temperatures. Indeed, as evident from Figs. 4 and 5, the weak field susceptibility is sensitive to temperature down to 100 mK. For stronger fields, for which the Zeeman energy exceeds the temperature, almost all spins are polarized and susceptibility depends very weakly on temperature.

IV. COMPARISON WITH RECENT SEARCHES FOR THE STONER INSTABILITY

To the best of our knowledge, with the exception of Refs. 16,17, there is no reported experimental observation of Stoner instability in 2D systems. In particular, recent susceptibility measurements based on Sh-dH data,[15,18] carried out down to a critical density of a superb sample ($n_c=8\times10^{10}$ cm^{-2}), find a finite susceptibility in the whole density range, in agreement with our result. We therefore turn to careful examination of the arguments used in Refs. 16 and 17 to claim the observation of such an instability. Both references rely on the magnetoresistance measured as a function of in-plane magnetic field. At high densities the resistance grows approximately quadratically with the field up to some density dependent field. Then it saturates or at least becomes weakly field dependent. It is believed, that at these densities the saturation field corresponds to full spin polarization. This large positive magnetoresistance is generic to all samples that show the so-called metallic phase in 2D and is, hence, very likely to provide an important clue for the understanding of the latter phenomenon. The authors of Refs. 16 and 17 have noticed that normalized magnetoresistance curves $\rho(n,B)/\rho(n,0)$ (magnetoconductance in the case of 17), measured at different densities, can be collapsed onto a single curve if the field is scaled by a density dependent field $B_c(n)$ (we use the notation of Ref. 16; Ref. 17 utilizes a somewhat different analysis in the same spirit). Moreover, for high densities, where magnetoresistance saturation is observed, $B_c(n)$ can be set to the saturation field. At lower densities (still above n_c) the saturation can no longer be observed but a scaling field $B_c(n)$ can still be found, so that the curves collapse one on top of another. The authors of these references noticed that B_c vanishes approximately linearly when the density approaches n_c, namely, $B_c(n)\propto n-n_c$. They then argued that, since $B_c(n)$ corresponds to full spin polarization at high densities, it should also correspond to full polarization at lower densities, where magnetoresistance saturation is no longer observable. Following that logic all the way to the critical density, they concluded that the vanishing of $B_c(n)$ at some finite density must indicate spontaneous polarization at zero field, i.e., the long awaited Stoner instability. We can not exclude Stoner instability in the superb samples used in Refs. 16 and 17, but we can prove that the procedure used to conclude the instability is wrong. To that end we show in Fig. 6 that our data obey the same scaling as in Ref. 16. In anticipation of the same dependence of $B_c(n)$ upon density as in Ref. 16 we surmise $B_c(n)\propto n-n_0$ (inset to Fig. 6) and find that for $n_0=1.15\times10^{11}$ cm^{-2} all our scaled magnetoresistance curves collapse onto a single curve (Fig. 6). Following the arguments in Refs. 16 and 17 we could have concluded Stoner instability at n_0, but our direct magnetization measurements at that density show finite susceptibility. The same fact is also reflected in Fig. 3(b). If the high field magnetization is extrapolated to zero field (dashed line) one may have erroneously predicted instability. Carrying the measurements to smaller fields exclude that possibility. The wrong assumption of Refs. 16 and 17 is the identification of $B_c(n)$ with a full polarization at all densities. Some of the authors of Ref. 17 later restricted their conclusion to the nonexisting case of perfectly clean samples.[30]

In summary, we were able to measure the thermodynamic spin magnetization of strongly correlated 2D electrons in a

single 2D layer. Albeit the substantial enhancement of the low temperature susceptibility, no ferromagnetic instability was observed. Yet, at densities in the vicinity of the critical one we observe almost free-spin-like susceptibility, indicating nearly perfect compensation of the kinetic energy by the ferromagnetic interaction. The possible relation between the large spin susceptibility at the critical density and the transition to strong localization calls for further theoretical and experimental studies. Understanding the role and nature of the localized spins might also turn to be important.

ACKNOWLEDGMENTS

We have benefited greatly from valuable discussions with A. Finkelstein, A. Stern, A. Kamenev, and V. Dolgopolov. This work was supported by the Israeli National Science Foundation, the DIP foundation and INTAS. V.P. was supported by NATO, NSF, INTAS, and Russian programs RFBR, ''Physics of nanostructures,'' ''Integration of education and academic research,'' ''The State support of leading scientific schools.''

[1] G. Senatore *et al.*, Solid State Commun. **119**, 333 (2001).
[2] C. Attaccalite, S. Moroni, P. Gori-Giorgi, and G. B. Bachelet, Phys. Rev. Lett. **88**, 256601 (2002).
[3] See, e.g., S. Doniach and E.H. Sondheimer, *Green's Functions for Solid State Physicists* (Benjamin, Reading, MA, 1974).
[4] B. Tanatar and D.M. Ceperley, Phys. Rev. B **39**, 5005 (1989).
[5] B. Bernu, L. Candido, and D. M. Ceperley, Phys. Rev. Lett. **86**, 870 (2001).
[6] K. Voelker and S. Chakravarty, Phys. Rev. B **64**, 235125 (2001).
[7] E. Abrahams, P. W. Anderson, D. C. Licciardello, and T. V. Ramakrishnan, Phys. Rev. Lett. **42**, 673 (1979).
[8] B. L. Altshuler and A. G. Aronov, in *Electron-electron Interactions in Disordered Systems*, edited by A. L. Efros and M. Pollak (Elsevier, Amsterdam, 1985), p. 1.
[9] A. M. Finkelstein, Sov. Phys. JETP **57**, 97 (1983).
[10] Gàbor Zala, B.N. Narozhny, and I.L. Aleiner, Phys. Rev. B **64**, 201201 (2001).
[11] A. Punnoose and A. M. Finkelstein, Phys. Rev. Lett. **88**, 016802 (2001); Physica A **302**, 318 (2001).
[12] F. F. Fang and P. J. Stiles, Phys. Rev. **174**, 823 (1968).
[13] T. Okamoto, K. Hosoya, S. Kawaji, and A. Yagi, Phys. Rev. Lett. **82**, 3875 (1999).
[14] S. A. Vitkalov, H. Zheng, K. M. Mertes, M. P. Sarachik, and T. M. Klapwijk, Phys. Rev. Lett. **85**, 2164 (2000).
[15] V. M. Pudalov, M. E. Gershenson, H. Kojima, N. Butch, E. M. Dizhur, G. Brunthaler, A. Prinz, G. Bauer, Phys. Rev. Lett. **88**, 196404 (2002).
[16] A. A. Shashkin, S. V. Kravchenko, V. T. Dolgopolov, and T. M. Klapwijk, Phys. Rev. Lett. **87**, 86801 (2001).
[17] S. A. Vitkalov, H. Zheng, K. M. Mertes, M. P. Sarachik, and T. M. Klapwijk, Phys. Rev. Lett. **87**, 086401 (2001).
[18] V. Pudalov, M. E. Gershenson, and H. Kojima, cond-mat/0110160 (unpublished).
[19] I. Meinel, D. Grundler, S. Bargstädt-Franke, C. Heyn, D. Heitmann, and B. David, Appl. Phys. Lett. **70**, 3305 (1997).
[20] J. G. E. Harris, D. D. Awschalom, K. D. Maranowski, and A. C. Gossard, J. Appl. Phys. **87**, 5102 (2000).
[21] S. V. Kravchenko, G. V. Kravchenko, J. E. Furneaux, V. M. Pudalov, and M. D'Iorio, Phys. Rev. B **50**, 8039 (1994).
[22] S. V. Kravchenko *et al.*, Phys. Rev. B **51**, 7038 (1995).
[23] O. Prus, M. Reznikov, U. Sivan, and V. Pudalov, Phys. Rev. Lett. **88**, 016801 (2002).
[24] E. Abrahams, S. V. Kravchenko, and M. P. Sarachik, Rev. Mod. Phys. **73**, 251 (2001).
[25] R. N. Bhatt and P. A. Lee, Phys. Rev. Lett. **48**, 344 (1982).
[26] V. M. Pudalov, G. Brunthaler, A. Prinz, and G. Bauer, JETP Lett. **65**, 932 (1997).
[27] D. Simonian, S. V. Kravchenko, M. P. Sarachik, and V. M. Pudalov, Phys. Rev. Lett. **79**, 2304 (1997).
[28] N. F. Mott, *Metal-Insulator Transitions* (Taylor & Francis, London, 1990).
[29] A. Gold and V. T. Dolgopolov, J. Phys.: Condens. Matter **14**, 7091 (2002).
[30] S. A. Vitkalov, M. P. Sarachik, and T. M. Klapwijk, Phys. Rev. B **65**, 201106 (2020).